Title
Relative Fixation Strength of Rabbit Subscapularis Repair Is Comparable to Human Supraspinatus Repair at Time 0

Journal
Clinical Orthopaedics and Related Research®, 472(8)

ISSN
0009-921X

Authors
Otarodifard, Karimdad
Wong, Jeffrey
Preston, Charles F
et al.

Publication Date
2014-08-01

DOI
10.1007/s11999-013-3439-z

Peer reviewed

Clin Orthop Relat Res (2014) 472:2440–2447
DOI 10.1007/s11999-013-3439-z

Clinical Orthopaedics and Related Research®
A Publication of The Association of Bone and Joint Surgeons®

SYMPOSIUM: SURGERY AND SCIENCE OF THE ROTATOR CUFF

Relative Fixation Strength of Rabbit Subscapularis Repair Is Comparable to Human Supraspinatus Repair at Time 0

Karimdad Otarodifard MD, Jeffrey Wong MD, Charles F. Preston MD, James E. Tibone MD, Thay Q. Lee PhD

Published online: 3 January 2014

Abstract

Background Recent evidence suggests that the rabbit subscapularis tendon may be anatomically, biomechanically, and histologically suitable to study rotator cuff pathology and repair. However, biomechanical comparisons of rotator cuff repairs in this model have not been evaluated and compared to those in human cadaveric specimens.

Questions/purposes We quantified the biomechanical properties of the repaired rabbit subscapularis tendon after (1) single-row, (2) double-row, and (3) transosseous-equivalent rotator cuff repair techniques and compared the ratios of repairs to previously published data for human repairs.

Methods Tensile testing was performed on 21 New Zealand White rabbit subscapularis tendon-humerus complexes for single-row repair, double-row repair, and transosseous-equivalent repair ($n = 7$ for each group). Video digitizing software was used to quantify deformation. Load elongation data were then used to quantify structural properties. We compared the ratios of rotator cuff repairs for the rabbit data to data from human supraspinatus repair studies previously performed in our laboratory. For our primary end points (linear stiffness, yield load, ultimate load, and energy absorbed to failure), with the numbers available, our statistical power to detect a clinically important difference (defined as 15%) was 85%.

Results The ratios of single-row/double-row repair were 0.72, 0.73, 0.71, and 0.66 for human supraspinatus and 0.77, 0.74, 0.79, and 0.89 for rabbit subscapularis repair for linear stiffness, yield load, ultimate load, and energy absorbed to failure, respectively. The ratios of double-row/transosseous-equivalent repair were 1.0, 0.86, 0.70, and 0.41 for human supraspinatus and 1.22, 0.85, 0.76, and 0.60 for rabbit subscapularis for linear stiffness, yield load, ultimate load, and energy absorbed to failure, respectively. There were no differences comparing rabbit to human repair ratios for any parameter ($p > 0.09$ for all comparisons).

Conclusions Subscapularis repairs in the rabbit at Time 0 result in comparable ratios to human supraspinatus repairs.

Clinical Relevance The biomechanical similarities between the different types of rotator cuff repair in the rabbit subscapularis and human supraspinatus at Time 0 provide more evidence that the rabbit subscapularis may be an appropriate model to study rotator cuff repairs.

The institution of one or more authors (KO, JW, TQL) has received funding, during the study period, from a grant from the VA Rehabilitation Research and Development Merit Review.
All ICMJE Conflict of Interest Forms for authors and *Clinical Orthopaedics and Related Research* editors and board members are on file with the publication and can be viewed on request.
Each author certifies that his or her institution approved the animal protocol for this investigation and that all investigations were conducted in conformity with ethical principles of research.
This work was performed at the Orthopaedic Biomechanics Laboratory, Long Beach VA Healthcare System, Long Beach, CA, USA.

K. Otarodifard, J. Wong, T. Q. Lee (✉)
Orthopaedic Biomechanics Laboratory, Long Beach VA Healthcare System (09/151), 5901 East 7th Street, Long Beach, CA 90822, USA
e-mail: tqlee@med.va.gov; tqlee@uci.edu

K. Otarodifard, J. Wong, T. Q. Lee
University of California, Irvine, CA, USA

K. Otarodifard, C. F. Preston, J. E. Tibone
Department of Orthopaedic Surgery, University of Southern California, Los Angeles, CA, USA

Introduction

To date, persistent tear rates after rotator cuff repair remain remarkably high, with recurrent tears requiring revision surgery occurring in 30% and 90% of supraspinatus and multitendon tears, respectively [14, 16, 17, 19, 22]. Multiple factors are thought to influence healing after cuff repair, including initial fixation strength [10], tendon-footprint contact area and pressure [4, 32, 34, 35, 44], tendon-footprint interface motion [1], tendon and bone tissue quality [19, 43], synovial fluid extravasation [2], and blood supply to the repair [15]. Development of an appropriate animal model could help in elucidating the relationship between these variables and healing.

In humans, most rotator cuff tears involve the supraspinatus tendon [28, 41, 45] and occur as a result of intrinsic and extrinsic factors affecting the tendon throughout life. Whereas intrinsic factors increase tendon susceptibility to injury, extrinsic factors are related to repetitive microtrauma associated with overuse [7, 23, 24, 36, 39]. A major factor contributing to this overuse tendinopathy is irritation of the tendon as it passes through a tunnel created by the coracoacromial arch during humeral elevation [5, 13, 29]. Based on the aforementioned criteria, an ideal animal model for rotator cuff pathology would closely recreate this extrinsic interaction between the tendon and its surrounding bony architecture.

Recent evidence suggests that the rabbit subscapularis tendon may be anatomically, biomechanically, and histologically suitable to study human rotator cuff pathology and repair [21]. The tendon passes under a tunnel composed laterally by the supraglenoidale tuberculum, medially by the coracobrachialis muscle, inferiorly by the infraglenoidale tuberculum, and superiorly by the coracoid processus before inserting on the lesser tubercle of the humerus. Furthermore, on detachment from its insertion, the muscle belly undergoes significant decreases in muscle mass and cross-sectional area, with fatty infiltration similar to that observed in humans after cuff tears [38]. In addition, the rabbit subscapularis footprint has been found to have dimensions of a mean 6.8 mm in the superior-inferior direction and 2.5 mm in the medial lateral direction, approximately ¼ of the size of the human supraspinatus footprint, which allows for recreation of human rotator cuff repair techniques in this model [20, 40].

Based on distinct anatomic, biomechanical, and histologic similarities, it is believed that the rabbit subscapularis complex may provide an appropriate model for the study of rotator cuff disease; however, the biomechanical differences of rotator cuff repairs in this model have not been evaluated or compared to human repairs. Therefore, we assessed the biomechanical characteristics of the rabbit subscapularis after (1) single-row, (2) double-row, and (3) transosseous-equivalent rotator cuff repair techniques and compared these findings to previously published data for human supraspinatus repairs. Specifically, we hypothesized that the initial biomechanical characteristics of these repairs will have relative properties similar to published data for supraspinatus rotator cuff repair performed in human cadaveric specimens.

Materials and Methods

Specimens

All work was approved by the Institutional Animal Care and Use Committee of our institution (Number 674: rabbit model for rotator cuff pathology). The shoulders of 21 fresh-frozen cadaveric New Zealand White rabbits carcasses obtained from Western Oregon Rabbit Co (Philomoth, OR, USA) were used. The rabbits were approximately 6 months of age and were males ranging in size from 3.4 to 3.8 kg [26]. The shoulder was dissected free of all muscular, ligamentous, and tendinous structures other than those of the rotator cuff. The infraspinatus, supraspinatus, and teres minor were released from the scapula and proximal humerus using sharp dissection. The subscapularis was subsequently dissected from its scapular origin with only its insertion on the proximal humerus left intact. Each subscapularis-tendon-bone complex was then randomly designated to a repair group (single row, double row, or transosseous equivalent; n = 7 for each group). The subscapularis tendon was released from its insertion and repaired according to its predetermined fixation group. Specimens were kept moist with normal saline solution during all phases of dissection, preparation, and testing.

Repair Techniques

All repair techniques utilized 1.3-mm Micro QUICKANCHOR® suture anchors single-loaded with Number 3/0 (2 metric) ORTHOCORD® suture (DePuy Mitek, Raynham, MA, USA). These devices have been approved by the FDA for use as described in this article. Standard knot tying was performed for all repairs, consisting of a standard sliding knot followed by three reversed half hitches.

For single-row repair, two suture anchors were placed 4 to 5 mm apart anterior to posterior on top of the far lateral tuberosity. Before anchor placement, pilot holes were drilled perpendicular to the articular surface using a 1.3-mm drill bit (Depuy Mitek). Simple suture configurations were utilized with the suture passes placed approximately 3 mm directly medial from the lateral tendon edge. A standard knot was utilized to fix the tendon directly over the native footprint (Fig. 1).

For double-row repair, two single-loaded suture anchors were placed approximately 4 to 5 mm apart from one another anterior to posterior at the far medial footprint

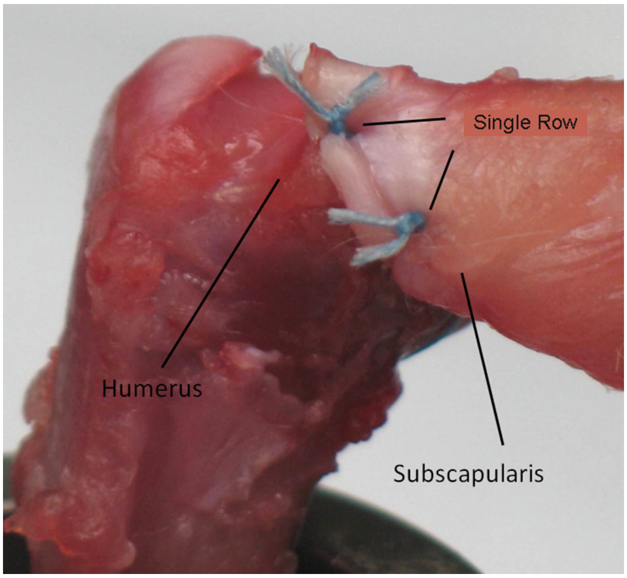

Fig. 1 Single-row repair of the rabbit subscapularis tendon is shown.

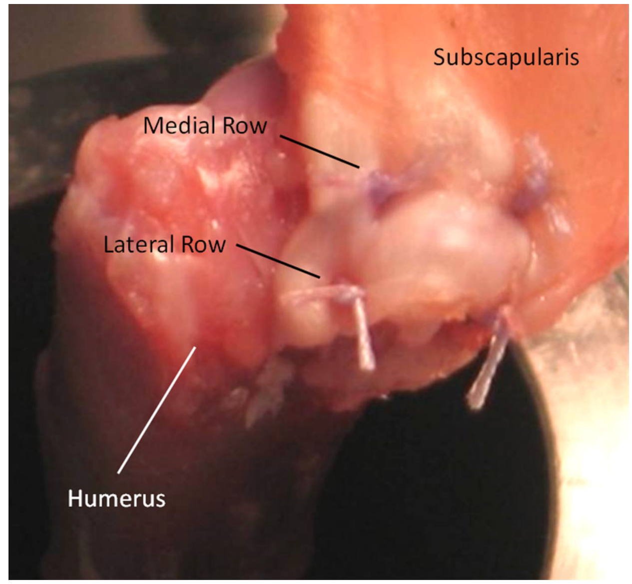

Fig. 2 Double-row repair of the rabbit subscapularis tendon is shown.

margin (2–3 mm medial from the tendon edge). Two additional anchors were then placed as far laterally on the lesser tuberosity as possible, allowing for maximum footprint coverage. Before anchor placement, pilot holes were drilled perpendicular to the articular surface using a 1.3-mm drill bit. Mattress suture configurations were employed to fix the tendon at the medial row, with sutures being passed through the tendon centered over each medial anchor; the suture passes were 3 mm apart from each other for a given anchor. Standard knot tying was utilized. Once the medial row was secured, the suture limbs were cut. The lateral tendon edge was then fixed using simple suture configurations, with each suture being passed directly lateral and in line with the medial row. The same standard knot tying technique was used, similar to what is done clinically in human patients (Fig. 2).

For transosseous-equivalent repair [33], the tendon was fixed at the medial edge of the native subscapularis footprint in the same fashion as described above for the double-row repair, with the anterior and posterior anchors placed at the far medial footprint adjacent to the articular surface 4 to 5 mm apart from one another. However, unlike the double-row repair, the medial suture limbs were not cut after they were tied. Instead, one suture limb from the medial row was passed through the eyelet of another free anchor. This anchor was then implanted laterally approximately 5 mm distal to the lateral edge of the rabbit subscapularis attachment site on the tuberosity. This suture limb, now incorporated into the lateral anchor, was tensioned and tied to a suture limb from the other medial anchor. A standard knot was used to compress the tendon against the footprint. The same process was then repeated using the two limbs remaining from the anterior and posterior medial anchors. The final configuration created an M suture crossing pattern on top of the repaired tendon. The lateral row of anchors was placed in line with the medial row of anchors 4 to 5 mm apart as well (Fig. 3).

Biomechanical Testing

Each subscapularis tendon-bone complex was subjected to uniaxial tensile testing using an Instron® testing apparatus (Instron, Norwood, MA, USA) with a 5-kN load cell while construct deformation was captured using a WINanalyze video digitizing system (Mikromak Service, Berlin, Germany). First, each subscapularis complex was potted into a custom testing jig using plaster of paris. The humerus was potted such that the angle between the humeral shaft and direction of tensile loading would approximate 120° to place the direction of pull grossly in line with the native rabbit subscapularis muscle fibers axis of contraction. To minimize soft tissue slippage during loading, the free end of the subscapularis tendon complex was secured to a custom soft tissue cryoclamp [9]. A Number 3/0 Monocryl™ suture (Ethicon, Inc, Somerville, NJ, USA) was placed into the subscapularis muscle belly using a Krackow stitch configuration to facilitate reproducible loading within this clamp. Once the subscapularis tendon complex was secured within the custom jig, markers were placed onto the anterior surface of the complex. One marker was placed on the clamp and the other was placed on the humeral head for later video analysis of construct deformation during loading (Fig. 4). This was done to eliminate any motion between the bone and potting.

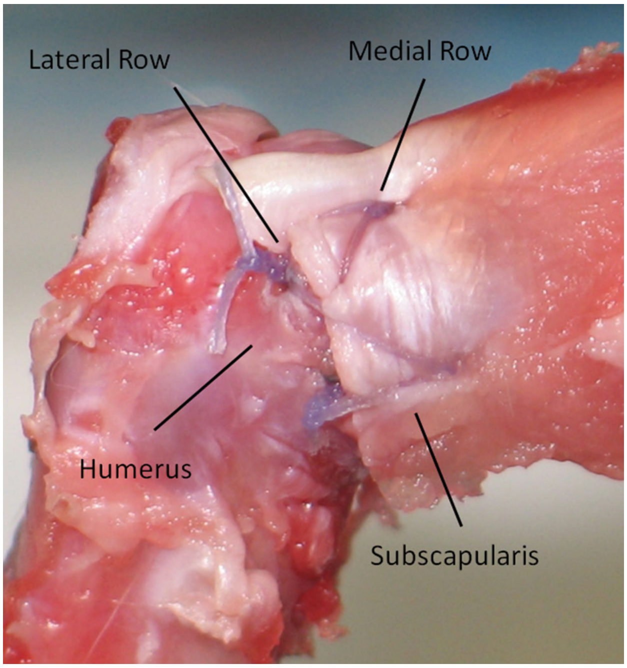

Fig. 3 Transosseous-equivalent repair of the rabbit subscapularis tendon is shown.

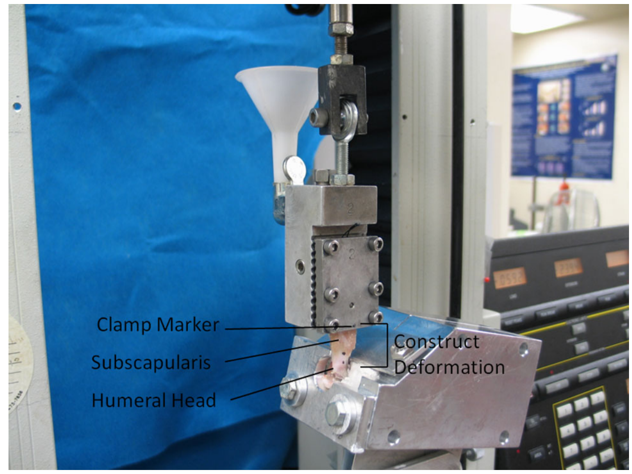

Fig. 4 The custom testing jig and Instron® testing apparatus are shown. The humerus was potted in an aluminum mounting fixture and the angle could be changed to ensure appropriate alignment of the construct for tensile testing. Markers on the clamp and humeral head were used to measure displacement of the construct to eliminate any motion occurring between the bone and the potting.

After positioning, liquid nitrogen was applied to the subscapularis muscle belly via the cryoclamp. The muscle was allowed to freeze for approximately 3 minutes and was subsequently subjected to uniaxial tensile testing. First, a 5-N preload was applied to the specimens for 30 seconds. The tendon was then cycled five times at amplitude of 1-mm displacement and a rate of 10 mm/minute. The tendon was then loaded to failure at a rate of 10 mm/minute. Data were recorded at 10 points/second. The failure was recorded using a high-resolution digital video camera. Construct deformation recorded from this video was analyzed using the WINanalyze video digitizing system, which tracked changes in displacement according to displacement of markers placed at the humeral head and Instron® clamp. Using Instron® load measurements and WINanalyze analysis of construct deformation, we determined the structural properties of repaired rabbit subscapularis complexes, including stiffness, yield load, ultimate load, and energy absorbed to failure.

Human Comparative Data

These findings in the rabbit model were compared to data from previously published human cadaveric studies to assess whether human rotator cuff repair techniques could be performed in the rabbit subscapularis and result in relative initial biomechanical fixation strength similar to that in human cadaveric repairs. Published studies evaluating human cadaveric supraspinatus repair performed in our laboratory were used for the comparisons. One study compared single-row to double-row repair [27] and the other double-row to transosseous-equivalent supraspinatus repair [35]. These studies used testing methodology similar to that used in the current study, and since they were performed in our laboratory, each specimen's individual data could be used for calculating ratios between the two repair techniques so that statistical comparisons could be performed. The ratio for each comparison was calculated from the same study since these were matched-pair cadaveric studies. We then could compare ratios of single-row to double-row repair and ratios of double-row to transosseous-equivalent repair between rabbits and humans.

Statistical Comparisons and Analyses

The ratios of each biomechanical parameter for single-row/double-row repairs and double-row/transosseous-equivalent repairs were calculated. All data were checked for normality using the Kolmogorov-Smirnov test ($p > 0.14$ for all parameters). Ratios of the rabbit subscapularis repairs were then compared to ratios of the human supraspinatus repairs using a one-way ANOVA with significance set at $\alpha = 0.05$ (Statistica®; StatSoft, Inc, Tulsa, OK, USA).

A power calculation for our primary end points (linear stiffness, yield load, ultimate load, and energy absorbed to failure) revealed that, with the numbers available, our statistical power to detect a clinically important difference (defined as 15%) was 85%.

Table 1. Structural properties of rotator cuff repair techniques in the rabbit subscapularis and previously published human cadaveric supraspinatus

Repair	Linear stiffness (N/mm)	Yield load (N)	Ultimate load (N)	Energy absorbed to failure (Nmm)
Rabbit subscapularis repair				
Single row	8.1 ± 2.3	21.7 ± 4.6	26.5 ± 5.1	60.5 ± 28.7
Double row	11.9 ± 5.6	32.7 ± 9.8	37.8 ± 11.6	90.4 ± 27.7
Transosseous equivalent	11.2 ± 3.6	40.1 ± 9.4	52.5 ± 9.3	159.8 ± 35.7
Human supraspinatus repair				
Single row vs double row (Kim et al. [27])				
Single row	81.3 ± 22.6	265.3 ± 70.0	349.7 ± 75.1	1419.4 ± 819.4
Double row	118.4 ± 15.0	371.0 ± 59.7	516.3 ± 120.8	2407.6 ± 1152.9
Double row vs transosseous equivalent (Park et al. [35])				
Double row	69.6 ± 16.8	214.3 ± 31.1	299.2 ± 52.5	1190.5 ± 291.1
Transosseous equivalent	69.1 ± 15.2	260.3 ± 69.5	443.0 ± 87.8	3210.9 ± 1055.7

Values are expressed as mean ± SD.

Table 2. Biomechanical fixation strength ratios (single row/double row and double row/transosseous equivalent) for the rabbit subscapularis rotator cuff repair compared to the cadaveric human supraspinatus repair

Variable	Single-row/double-row ratio			Double-row/transosseous-equivalent ratio		
	Rabbit	Human (Kim et al. [27])	p value	Rabbit	Human (Park et al. [35])	p value
Linear stiffness	0.77 ± 0.29	0.72 ± 0.28	0.73	1.22 ± 0.76	1.00 ± 0.06	0.49
Yield load	0.74 ± 0.36	0.73 ± 0.23	0.95	0.85 ± 0.31	0.86 ± 0.23	0.93
Ultimate load	0.79 ± 0.38	0.71 ± 0.20	0.61	0.76 ± 0.32	0.70 ± 0.22	0.72
Energy absorbed to failure	0.89 ± 0.88	0.66 ± 0.31	0.50	0.60 ± 0.22	0.41 ± 0.15	0.09

Values are expressed as mean ± SD.

Results

Single-row/Double-row Comparisons

There were no differences in the biomechanical characteristics for the rabbit versus human comparisons of single-row/double-row ratios ($p > 0.50$ for all comparisons) (Table 1). The ratios of single-row/double-row fixation for the human supraspinatus repairs were 0.72 for linear stiffness, 0.73 for yield load, 0.71 for ultimate load, and 0.66 for energy absorbed to failure. In the rabbit subscapularis repair, these ratios were 0.77 for linear stiffness, 0.74 for yield load, 0.79 for ultimate load, and 0.89 for energy absorbed at failure [27] (Table 2).

Double-row/Transosseous-equivalent Comparisons

With the numbers available, there were no differences for the rabbit versus human comparisons of double-row/transosseous-equivalent ratios ($p > 0.09$ for all comparisons). The ratios of double-row/transosseous-equivalent fixation for the human supraspinatus repairs were 1.00 for linear stiffness, 0.86 for yield load, 0.70 for ultimate load, and 0.41 for energy absorbed to failure. In the rabbit subscapularis repair, the ratios of double-row/transosseous-equivalent repair were 1.22 for linear stiffness, 0.85 for yield load, 0.76 for ultimate load, and 0.60 for energy absorbed at failure [35] (Table 2).

Discussion

Many factors are thought to play a role in the pathogenesis of human chronic supraspinatus tears, with both intrinsic changes within the tendon and extrinsic influences of the tendons surrounding skeletal architecture believed to contribute to its etiology [1, 2, 4, 10, 19, 43, 44]. To ultimately advance therapeutic intervention, development of an appropriate animal model allowing in vivo simulation of rotator cuff disease and exploration of the factors affecting its repair is essential. The purpose of this investigation was to further validate the novel rabbit subscapularis tendon model as a viable alternative for the study of human rotator cuff repair. Specifically, because initial fixation strength is a major factor limiting tendon-footprint interface motion and facilitating healing, we assessed the initial biomechanical fixation characteristics of rotator cuff repairs in the rabbit model and compared these relative properties to those in human cadaveric cuff repairs.

There are several limitations to this study. Most importantly, correlations between rabbit and human rotator cuff repair strengths made in this investigation were not based on direct experimental comparisons. Information obtained from this study was extrapolated to data previously published. Thus, variations in surgical technique, sample sizes, and experimental protocols from this investigation and those performed in humans must be taken into account when assessing the validity of our conclusions. However, the human supraspinatus repair studies were performed in our laboratory and therefore we were able to compare the averages of each specimen's results from matched-pair studies. Furthermore, previously published data for double-row fixation strength differed between the two different studies (Table 1). This difference likely resulted from differences in specimen group, anchor material, and experimental protocol between the studies and further highlights that the presence of confounding variables must be taken into account when interpreting these results; therefore, we calculated ratios for repair techniques for the human studies only within each matched-pair study. This study also only evaluated the biomechanical properties of the repair constructs at Time 0; it is not known how healing in the rabbit model compares to human healing as the repaired shoulder in the rabbit, as a quadruped, will experience weightbearing loads uncommon in healing human shoulders, likely affecting healing response. Furthermore, difficulty with postoperative immobilization may further complicate postoperative tendon-footprint healing and influence ultimate outcomes. Another limitation of this study is the small sample size; however, there was only one parameter approaching statistical significance ($p = 0.09$) and post hoc power analysis revealed 50% power to detect a significant difference for this parameter. However, given the available alternatives, the rabbit subscapularis is an option for use as an animal model to evaluate rotator cuff repair.

When compared to published cadaveric supraspinatus repair data [27, 35], comparable differences in initial biomechanical fixation strength between different cuff repair techniques were observed in the rabbit subscapularis tendon model, showing that human repair techniques could be reproduced in the rabbit subscapularis model without substantially altering the biomechanical characteristics of the repairs.

Many animals including rats, rabbits, dogs, and sheep have been used in the study of rotator cuff disease and repair [3, 6, 11, 18, 42]. Although the large glenohumeral joints of dogs and sheep provide an advantage for performing rotator cuff repair, the acromioclavicular structural anatomy in these species does not cover the humeral head and rotator cuff. The rat supraspinatus on the other hand has been shown to pass under a fibroosseous tunnel during forward locomotion [42]. However, the rat supraspinatus is muscular rather than tendinous as it passes through this tunnel and thus the point of impingement during humeral elevation is on the muscle belly, not the tendon. The rat supraspinatus also does not undergo histologic changes comparable to those seen in the human supraspinatus after injury, and the size of the rat model makes it impossible to perform repair techniques similar to those performed in humans [6]. In the rabbit supraspinatus tendon, fatty infiltration and atrophy appear after injury [8, 12] and human rotator cuff repair techniques have been performed in this model with biomechanical outcomes similar to those expected for human cuffs [31]. However, the tendon does not pass under any type of bony or ligamentous arch during motion as does the rabbit subscapularis tendon.

Given the relative biomechanical similarities between repair constructs in the human supraspinatus to those in the rabbit subscapularis and the previously noted similarities in surrounding osseoligamentous environment and tendon response to injury, the rabbit subscapularis tendon provides a viable animal model for studying the factors affecting cuff repair and healing. By performing in vivo studies using the rabbit subscapularis tendon, histologic analysis coupled with biomechanical testing can be used to elucidate which repair techniques would ultimately result in improved healing of the rotator cuff. Furthermore, there is growing interest in the efficacy of biologic augmentation with platelet-rich plasma, bone marrow aspirate, growth factor supplements, scaffolds, and gene-modified cell therapy for enhancing intrinsic healing potential of repaired tendons [25, 30, 37], which could also be studied with this model. In conclusion, commonly used rotator cuff repair techniques can be recreated in the rabbit subscapularis with relative Time 0 results similar to human cadaveric data. This observation combined with the unique anatomic [20, 21], histologic [38], and biomechanical similarities between the human supraspinatus and rabbit subscapularis provides evidence that the rabbit subscapularis is a viable animal model to study rotator cuff pathology.

Acknowledgments The authors acknowledge Ranjan Gupta MD and Maxwell Park MD for their expertise and involvement in the development of this animal model for rotator cuff pathology.

References

1. Ahmad CS, Stewart AM, Izquierdo R, Bigliani LU. Tendon-bone interface motion in transosseous suture and suture anchor rotator cuff repair techniques. *Am J Sports Med.* 2005;33:1667–1671.

2. Ahmad CS, Vorys GC, Covey A, Levine WN, Gardner TR, Bigliani LU. Rotator cuff repair fluid extravasation characteristics are influenced by repair technique. *J Shoulder Elbow Surg*. 2009;18:976–981.
3. Aoki M, Oguma H, Fukushima S, Ishii S, Ohtani S, Murakami G. Fibrous connection to bone after immediate repair of the canine infraspinatus: the most effective bony surface for tendon attachment. *J Shoulder Elbow Surg*. 2001;10:123–128.
4. Apreleva M, Ozbaydar M, Fitzgibbons PG, Warner JJ. Rotator cuff tears: the effect of the reconstruction method on three-dimensional repair site area. *Arthroscopy*. 2002;18:519–526.
5. Banas MP, Miller RJ, Totterman S. Relationship between the lateral acromion angle and rotator cuff disease. *J Shoulder Elbow Surg*. 1995;4:454–461.
6. Barton ER, Gimbel JA, Williams GR, Soslowsky LJ. Rat supraspinatus muscle atrophy after tendon detachment. *J Orthop Res*. 2005;23:259–265.
7. Bigliani LU, Ticker JB, Flatow EL, Soslowsky LJ, Mow VC. The relationship of acromial architecture to rotator cuff disease. *Clin Sports Med*. 1991;10:823–838.
8. Bjorkenheim JM. Structure and function of the rabbit's supraspinatus muscle after resection of its tendon. *Acta Orthop Scand*. 1989;60:461–463.
9. Bowser JE, Elder SH, Rashmir-Raven AM, Swiderski CE. A cryogenic clamping technique that facilitates ultimate tensile strength determinations in tendons and ligaments. *Vet Comp Orthop Traumatol*. 2011;24:370–373.
10. Burkhart SS, Lo IK. Arthroscopic rotator cuff repair. *J Am Acad Orthop Surg*. 2006;14:333–346.
11. Coleman SH, Fealy S, Ehteshami JR, MacGillivray JD, Altchek DW, Warren RF, Turner AS. Chronic rotator cuff injury and repair model in sheep. *J Bone Joint Surg Am*. 2003;85:2391–2402.
12. Fabis J, Kordek P, Bogucki A, Mazanowska-Gajdowicz J. Function of the rabbit supraspinatus muscle after large detachment of its tendon: 6-week, 3-month, and 6-month observation. *J Shoulder Elbow Surg*. 2000;9:211–216.
13. Flatow EL, Soslowsky LJ, Ticker JB, Pawluk RJ, Hepler M, Ark J, Mow VC, Bigliani LU. Excursion of the rotator cuff under the acromion: patterns of subacromial contact. *Am J Sports Med*. 1994;22:779–788.
14. Galatz LM, Ball CM, Teefey SA, Middleton WD, Yamaguchi K. The outcome and repair integrity of completely arthroscopically repaired large and massive rotator cuff tears. *J Bone Joint Surg Am*. 2004;86:219–224.
15. Gamradt SC, Gallo RA, Adler RS, Maderazo A, Altchek DW, Warren RF, Fealy S. Vascularity of the supraspinatus tendon three months after repair: characterization using contrast-enhanced ultrasound. *J Shoulder Elbow Surg*. 2010;19:73–80.
16. Gazielly DF, Gleyze P, Montagnon C. Functional and anatomical results after rotator cuff repair. *Clin Orthop Relat Res*. 1994;304:43–53.
17. Gerber C, Fuchs B, Hodler J. The results of repair of massive tears of the rotator cuff. *J Bone Joint Surg Am*. 2000;82:505–515.
18. Gerber C, Meyer DC, Frey E, von Rechenberg B, Hoppeler H, Frigg R, Jost B, Zumstein MA. Neer Award 2007. Reversion of structural muscle changes caused by chronic rotator cuff tears using continuous musculotendinous traction: an experimental study in sheep. *J Shoulder Elbow Surg*. 2009;18:163–171.
19. Goutallier D, Postel JM, Gleyze P, Leguilloux P, Van Driessche S. Influence of cuff muscle fatty degeneration on anatomic and functional outcomes after simple suture of full-thickness tears. *J Shoulder Elbow Surg*. 2003;12:550–554.
20. Grumet RC, Hadley S, Diltz MV, Lee TQ, Gupta R. Development of a new model for rotator cuff pathology: the rabbit subscapularis muscle. *Acta Orthop*. 2009;80:97–103.
21. Gupta R, Lee TQ. Contributions of the different rabbit models to our understanding of rotator cuff pathology. *J Shoulder Elbow Surg*. 2007;16(5 suppl):S149–S157.
22. Harryman DT 2nd, Mack LA, Wang KY, Jackins SE, Richardson ML, Matsen FA 3rd. Repairs of the rotator cuff: correlation of functional results with integrity of the cuff. *J Bone Joint Surg Am*. 1991;73:982–989.
23. Hashimoto T, Nobuhara K, Hamada T. Pathologic evidence of degeneration as a primary cause of rotator cuff tear. *Clin Orthop Relat Res*. 2003;415:111–120.
24. Irlenbusch U, Gansen HK. Muscle biopsy investigations on neuromuscular insufficiency of the rotator cuff: a contribution to the functional impingement of the shoulder joint. *J Shoulder Elbow Surg*. 2003;12:422–426.
25. Isaac C, Gharaibeh B, Witt M, Wright VJ, Huard J. Biologic approaches to enhance rotator cuff healing after injury. *J Shoulder Elbow Surg*. 2012;21:181–190.
26. Isaksson H, Harjula T, Koistinen A, Iivarinen J, Seppanen K, Arokoski JP, Brama PA, Jurvelin JS, Helminen HJ. Collagen and mineral deposition in rabbit cortical bone during maturation and growth: effects on tissue properties. *J Orthop Res*. 2010;28:1626–1633.
27. Kim DH, Elattrache NS, Tibone JE, Jun BJ, DeLaMora SN, Kvitne RS, Lee TQ. Biomechanical comparison of a single-row versus double-row suture anchor technique for rotator cuff repair. *Am J Sports Med*. 2006;34:407–414.
28. Milgrom C, Schaffler M, Gilbert S, van Holsbeeck M. Rotator-cuff changes in asymptomatic adults: the effect of age, hand dominance and gender. *J Bone Joint Surg Br*. 1995;77:296–298.
29. Neer CS 2nd. Anterior acromioplasty for the chronic impingement syndrome in the shoulder: a preliminary report. *J Bone Joint Surg Am*. 1972;54:41–50.
30. Nixon AJ, Watts AE, Schnabel LV. Cell- and gene-based approaches to tendon regeneration. *J Shoulder Elbow Surg*. 2012;21:278–294.
31. Ozbaydar M, Elhassan B, Esenyel C, Atalar A, Bozdag E, Sunbuloglu E, Kopuz N, Demirhan M. A comparison of single-versus double-row suture anchor techniques in a simulated repair of the rotator cuff: an experimental study in rabbits. *J Bone Joint Surg Br*. 2008;90:1386–1391.
32. Park MC, Cadet ER, Levine WN, Bigliani LU, Ahmad CS. Tendon-to-bone pressure distributions at a repaired rotator cuff footprint using transosseous suture and suture anchor fixation techniques. *Am J Sports Med*. 2005;33:1154–1159.
33. Park MC, Elattrache NS, Ahmad CS, Tibone JE. "Transosseous-equivalent" rotator cuff repair technique. *Arthroscopy*. 2006;22:1360.e1–5.
34. Park MC, ElAttrache NS, Tibone JE, Ahmad CS, Jun BJ, Lee TQ. Part I. Footprint contact characteristics for a transosseous-equivalent rotator cuff repair technique compared with a double-row repair technique. *J Shoulder Elbow Surg*. 2007;16:461–468.
35. Park MC, Tibone JE, ElAttrache NS, Ahmad CS, Jun BJ, Lee TQ. Part II. Biomechanical assessment for a footprint-restoring transosseous-equivalent rotator cuff repair technique compared with a double-row repair technique. *J Shoulder Elbow Surg*. 2007;16:469–476.
36. Reilly P, Amis AA, Wallace AL, Emery RJ. Supraspinatus tears: propagation and strain alteration. *J Shoulder Elbow Surg*. 2003;12:134–138.
37. Ricchetti ET, Aurora A, Iannotti JP, Derwin KA. Scaffold devices for rotator cuff repair. *J Shoulder Elbow Surg*. 2012;21:251–265.
38. Rowshan K, Hadley S, Pham K, Caiozzo V, Lee TQ, Gupta R. Development of fatty atrophy after neurologic and rotator cuff injuries in an animal model of rotator cuff pathology. *J Bone Joint Surg Am*. 2010;92:2270–2278.
39. Rudzki JR, Adler RS, Warren RF, Kadrmas WR, Verma N, Pearle AD, Lyman S, Fealy S. Contrast-enhanced ultrasound

characterization of the vascularity of the rotator cuff tendon: age- and activity-related changes in the intact asymptomatic rotator cuff. *J Shoulder Elbow Surg*. 2008;17:96S–100S.

40. Ruotolo C, Fow JE, Nottage WM. The supraspinatus footprint: an anatomic study of the supraspinatus insertion. *Arthroscopy*. 2004;20:246–249.
41. Sher JS, Uribe JW, Posada A, Murphy BJ, Zlatkin MB. Abnormal findings on magnetic resonance images of asymptomatic shoulders. *J Bone Joint Surg Am*. 1995;77:10–15.
42. Soslowsky LJ, Carpenter JE, DeBano CM, Banerji I, Moalli MR. Development and use of an animal model for investigations on rotator cuff disease. *J Shoulder Elbow Surg*. 1996;5:383–392.
43. Thomazeau H, Boukobza E, Morcet N, Chaperon J, Langlais F. Prediction of rotator cuff repair results by magnetic resonance imaging. *Clin Orthop Relat Res*. 1997;344:275–283.
44. Tuoheti Y, Itoi E, Yamamoto N, Seki N, Abe H, Minagawa H, Okada K, Shimada Y. Contact area, contact pressure, and pressure patterns of the tendon-bone interface after rotator cuff repair. *Am J Sports Med*. 2005;33:1869–1874.
45. Yamaguchi K, Ditsios K, Middleton WD, Hildebolt CF, Galatz LM, Teefey SA. The demographic and morphological features of rotator cuff disease: a comparison of asymptomatic and symptomatic shoulders. *J Bone Joint Surg Am*. 2006;88:1699–1704.